ABSTRACT

PHYSICS

Myers, Terry W. B.S. Southern University, 1988

TUNING WAVELENGTH SELECTIVE BIREFRINGENT OPTICAL FIBER FILTERS USING TWIST BIREFRINGENCE

Advisor: Dr. Charles S. Brown

Thesis dated May, 1991

A novel physical tuning mechanism for optical fiber filters is proposed and studied. To explore tuning mechanisms, a theoretical model of a Solc birefringent fiber filter is described. The coherency equation of motion for a birefringent filter is solved by transforming to the Stokes-Mueller matrix equation via the measurable Stokes parameters. The Mueller matrix is then expanded in a Taylor series using the generators of the Lorentz transformations. The Stokes vectors and Mueller matrices provide a theoretical formalism which is used to simulate an experimental set-up and to describe the transmission of light through a birefringent fiber filter system. Hence, the theoretical expression for the transmission spectra incident on a detector is derived. This expression is then transformed to the more convenient fourier series form. This form is used to determine the particular type of perturbation necessary to tune a filter. Specifically, a tuning mechanism utilizing twist birefringence is proposed

and analyzed. Moreover, we show using theoretical and computer simulation studies that twist birefringence tunes a filter spectra over a narrow but usable range, provided each stage in the filter is twisted at the same rate. For example, a twist birefringence of 85.7 rad/m generated a 42.8 nm tuning range on the filter spectra of a three-stage Solc-type fiber filter when each optical fiber stage is linearly birefringent with a beat length of 18.94 mm at 1282 nm.

TUNING WAVELENGTH SELECTIVE BIREFRINGENT OPTICAL FIBER FILTERS USING TWIST BIREFRINGENCE

A THESIS

SUBMITTED TO THE FACULTY OF CLARK ATLANTA UNIVERSITY

IN PARTIAL FULFILLMENT OF THE REQUIREMENTS FOR

THE DEGREE OF MASTER OF SCIENCE

BY

TERRY WAYNE MYERS

DEPARTMENT OF PHYSICS

ATLANTA, GEORGIA

MAY 1991

ACKNOWLEDGEMENT

I would like to thank Dr. Charles Brown, an AT&T visiting professor, for his assistance and guidance in the development of this project. I would also like to thank him for many hours of fruitful conversation concerning various topics in the areas of optics and fiber optics. All members of the physics department faculty and staff are acknowledged for their role in my educational and personal development. Special thanks goes out to Dr. Msezane for his continuous support of my graduate studies. Also, I would like to thank Dr. Rhodes for his meaningful discussions about various topics in optics. I would like to thank Julian Niles and all the graduate and undergraduate students that have supported me while I attended Clark Atlanta University. Finally, I would like to thank Dr. F. Sears for exposing me to different optical fiber splicing and characterization techniques.

TABLE OF CONTENTS

LIST OF FIGURES

CHAPTER I

INTRODUCTION

Over the past several years important developments have been made in the design and theory of birefringent optical filters. An optical filter is a device which transmits selected wavelengths of light while blocking others. Birefringent filters are devices that achieve this by inducing different evolutions of the state of polarization for each wavelength such that some wavelengths are passed or blocked at the exit polarizer. Initially, birefringent filters were developed for solar research. Since their invention in the 1930's, their use has expanded into several areas, such as optical fiber telecommunications, interferometric devices, integrated optical devices, and other high-tech areas. Up until the early part of the past decade, most filters were designed to pass fixed wavelengths (no tuning was possible). In 1975, Beckers and Carl Zeiss Corporation[1] developed the first tunable birefringent filter. Title and Rosenberg[2] later developed a technique to tune a birefringent filter over a broad spectral range. In addition, other tuning techniques were developed for use in birefringent filter systems.[3] All tuning methods utilize either direct or indirect mechanisms. A direct method, like the Fabry-Perot,[3] changes the medium to achieve tuning. An electro-optical technique,[2] another direct method, adjusts the retardation of birefringent elements of the filter. The

method developed by Title and Rosenberg, however, is an indirect method, since the birefringent medium is not perturbed but rather the output spectra is perturbed.

In this thesis, a direct physical tuning mechanism for wavelength selective birefringent optical fiber filters is proposed, modeled and analyzed. The elasto-optical effects of an optical fiber are exploited by using the circular birefringence induced by a physical twist to tune a linear birefringent single-mode fiber filter. To elaborate on these effects, a model for the single-mode fiber is described in chapter II. The Jones calculus[4] and Mueller matrix formalism are two of several techniques used to describe birefringence and the evolution of polarization (EOP) in optical components. Recently, Brown[5] used an operator formalism to derive the exact Mueller matrix for birefringence in closed form. In addition, Brown developed a formalism which is suitable for modeling actual experimental set-ups. This formalism is discussed in chapter II. The two classic types of birefringent filters, Lyot and Solc, are discussed and described in chapter III. In chapter IV, a proposed physical model for the twist-induced tunable wavelength selective birefringent filter is described and analyzed. Finally, in chapter V the advantages, disadvantages and applications of twist-induced tuning are discussed.

CHAPTER II

FORMALISM

The model of a cylindrical weakly guiding single-mode fiber with no absorption or perturbations along the propagation length is

$$\varepsilon(r,\phi) = \varepsilon_o(r) . \tag{1}$$

Here, $\varepsilon_o(r)$ characterizes an ideal cylindrically symmetric fiber.

Since only the propagating fields are of interest, the transverse electric field is considered. The transverse electric field is a two-component field. If it is assumed the ideal mode field vectors, $\mathscr{E}_m^t(r,\phi)$, form a two-component orthogonal set,[6] from which the ideal (unperturbed) transverse field can be expanded. These transverse fields of the ideal fiber are given by

$$\mathscr{E}_o^t(r,\phi,z) = \sum_{m=1}^{2} a_m \mathscr{E}_m^t(r,\phi)\, e^{i\beta_m z} . \tag{2}$$

Here, a_m is the constant amplitude of the m^{th} component of the transverse field, β_m is the propagation constant of the m^{th} polarization component, $e^{i\beta m z}$ is the phase factor associated with propagation of the m^{th} component in the z-

direction in an ideal fiber and $\mathscr{E}_m^t(r,\phi)$ is the m^{th} component of the transverse polarization unit vector which depends on r and ϕ. Since the polarization components of the ideal fiber are degenerate, they do not couple, hence, the state of polarization (SOP) is constant along the propagation length.

For the case where imperfections and perturbations are present in single-mode fibers, the dielectric permeability is

$$\varepsilon(r,\phi) = \varepsilon_o(r) + \tilde{\varepsilon}(r,\phi,z). \qquad (3)$$

Here, $\tilde{\varepsilon}(r,\phi,z)$ represents perturbations along the propagation direction, z, and can be a scalar (describing core deformation) or a tensor (describing stress anistropies and external fields). It is also assumed that this perturbation is small relative to $\varepsilon_o(r)$.

The SOP of the perturbed fiber, unlike the unperturbed fiber, evolves from state to state as light propagates along the fiber. This EOP is due to the coupling of the transverse polarization mode components via the perturbations. The transverse electric field for the perturbed case can be written in terms of the ideal modes as[7]

$$\mathcal{E}^t(r,\phi,z) = \sum_{m=1}^{2} a_m(z)\, \mathcal{E}_m^t(r,\phi)\, e^{i\beta_m z}. \tag{4}$$

Here, the coefficients, $a_m(z)$, are slowly varying and contain the effects of the perturbations. The SOP of the transverse field at a certain position, z, along the propagating path is determined by the phase and magnitude of $\mathcal{E}^t(r,\phi,z)$.

In order to describe mode propagation in the perturbed fiber theoretically, equation (4) is inserted into Maxwell's wave equation. This results in[8]

$$\sum_{m=1}^{2} e^{ik_m z}\Big[a_m(z)\,\nabla_t^2 \mathcal{E}_m^t(x,y) + \Big(\frac{\partial^2 a_m}{\partial z^2} + 2ik_m\frac{\partial^2 a_m}{\partial z^2} - k_m^2 a_m\Big)\mathcal{E}_m^t + \frac{\mu}{c^2}\omega^2(\tilde{\varepsilon}+\varepsilon_o)\,a_m(z)\,\mathcal{E}_m^t - \nabla_t\big(-\mathcal{E}_m^t\cdot\nabla_t \ln\varepsilon_o\big)\,a_m - \frac{\Big[\frac{\partial\tilde{\varepsilon}}{\partial z}\mathcal{E}_m a_m + \tilde{\varepsilon}\frac{\partial a_m}{\partial z}\mathcal{E}_m + (ik_m)\tilde{\varepsilon}\,\mathcal{E}_m a_m\Big]\cdot\vec{e}_z - \nabla_t\cdot(\tilde{\varepsilon}\,\mathcal{E}_m a_m)}{\varepsilon_o}\Big] = 0. \tag{5}$$

If all the terms in equation (5) that are 2nd order small or higher are neglected and use is made of the ideal mode equation,[8] then equation (5) is multiplied by $\varepsilon\nabla\mathcal{E}_n^t$. Using the orthogonality relation,

$$\int\int(\mathcal{E}_m^t\cdot(\varepsilon\nabla\mathcal{E}_n^t))^z dxdy = 0,\ m\neq n, \tag{6}$$

leads to a general first order set of differential equations for mode propagation along a perturbed fiber. This equation is called the coupled-mode equation, which is expressed as

$$\frac{da_n(z)}{dz} = iK_{mn}(z)\, a_m(z), \quad n = 1,2. \tag{7}$$

The $K_{mn}(z)$'s (see reference 8) are the elements of the coupling matrix and contain the integrals associated with the orthogonality relation.

The evolution of polarization (EOP) can be described by a two-component vector and a (2x2) matrix.[7] In abstract operator-vector language, the coupled-mode equations can be expressed as

$$\frac{d\vec{a}(z)}{dz} = i\hat{K}(z)\cdot\vec{a}(z). \tag{8}$$

Here, $\vec{a}(z)$ is a column vector,

$$\vec{a}(z) = \begin{pmatrix} a_1(z) \\ a_2(z) \end{pmatrix}, \tag{9}$$

representing the two orthogonal components of the perturbed field amplitudes, and $\hat{K}(z)$ is the (2x2) coupling operator, which is represented by

$$\hat{K}(z) = \begin{pmatrix} K_{11}(z) & K_{12}(z) \\ K_{21}(z) & K_{22}(z) \end{pmatrix}. \qquad (10)$$

For lossless transmission, $\hat{K}(z)$ is hermitian (i.e., $\hat{K}(z) = \hat{K}^{+}(z)$). Thus, $\hat{K}(z)$ represents birefringent effects only.

Since only measurable quantities are of interest here, (the field amplitudes are not measurable[9]) the coherency matrix (with measurable matrix elements[10]) is used. The coherency operator is defined as

$$\hat{I}(z) = \vec{a}(z) \cdot \vec{a}^{+}(z) . \qquad (11)$$

Upon taking the derivative with respect to the propagating length, z, we have

$$\frac{d\hat{I}(z)}{dz} = \vec{a}(z) \cdot \frac{d\vec{a}^{+}(z)}{dz} + \frac{d\vec{a}(z)}{dz} \cdot \vec{a}^{+}(z) . \qquad (12)$$

Now, substitute equation (8) and its complex conjugate into equation (12), then use the hermitian properties of $\hat{K}(z)$, the coherency equation of motion (CEM) becomes

$$\frac{d\hat{I}(z)}{dz} = i\,[\hat{K}(z), \hat{I}(z)] . \qquad (13)$$

Here, $[\hat{K}(z), \hat{I}(z)]$ is a commutator and is defined as

$[\hat{K}(z)\hat{I}(z) - \hat{I}(z)\hat{K}(z)]$. Equation (11) can be integrated using the z-order exponentials (see appendix A).[11] Using this method, the solution to the CEM is

$$\hat{I}(z) = (\underline{Z}\exp[i\int_0^z [\hat{K}(z'),\cdot]\, dz'])\cdot\hat{I}(z_o), \qquad (14)$$

where $[\hat{K}(z'),\cdot]\,\hat{I}(z) = [\underline{\hat{K}}(z'),\hat{I}(z)]$.[11]

To transform to Stokes space, the pauli spin matrices, which are associated with the SU(2) symmetry of the two-state field are used to expand[12] the (2x2) matrices. The coefficients of the expansion of the coherency operator, $\hat{I}(z)$, are the four Stokes parameters which describe polarization phenomena. The four Stokes parameters are given by s_o, s_1, s_2 and s_3. In terms of field amplitudes, the Stokes parameters are defined as

$$\begin{aligned} s_o &= a_1^2 + a_2^2, \\ s_1 &= a_1^2 - a_2^2, \\ s_2 &= 2a_1a_2\cos(\beta), \\ s_3 &= 2ia_1a_2\sin(\beta), \end{aligned} \qquad (15)$$

where a_1 and a_2 are the orthogonal components of the amplitudes of the transverse electric field and β is the magnitude of the birefringence. It is defined as $\beta=2\pi(n_1-n_2)/\lambda$, where n_1 and n_2 are the phase indices of refraction along the principal axes and λ is the free-space wavelength.

It is worth noting that in actual experiments, these parameters are time averaged.[13] Physically, the Stokes parameters have the following interpretation: s_0 is the sum of the squares of the amplitudes and therefore represents the total intensity, s_1 is the excess of parallel to perpendicular linearly polarized light, s_2 is the excess $\pm 45^\circ$ linearly polarized light with respect to the parallel or perpendicular axis and s_3 is the excess of right to left circularly polarized light. Equation (14) is transformed to the Stokes picture by using the following SU(2) representation

$$\hat{I}(z) = \tfrac{1}{2}\left(s_o(z)\,\hat{\sigma}_o + \vec{s}(z)\cdot\hat{\sigma},\right) \tag{16}$$

and

$$\hat{K}(z) = \tfrac{1}{2}\left(\beta_o(z)\,\hat{\sigma}_o + \vec{\beta}(z)\cdot\hat{\sigma},\right). \tag{17}$$

Here, $\hat{\sigma} = \hat{\sigma}_1\vec{e}_1 + \hat{\sigma}_2\vec{e}_2 + \hat{\sigma}_3\vec{e}_3$ (which are given in appendix B). Also, β_o denotes the unperturbed birefringence (which is assumed to be zero), and $\vec{\beta}(z)$ is the birefringence vector with $\beta_1(z)$, $\beta_2(z)$ and $\beta_3(z)$ representing the components of the birefringence in Stokes space.[12]

Utilizing equations (16) and (17) along with the pauli spin matrix algebra[14] and the additional assumption of constant birefringence, (i.e., β is independent of z) the

CEM for birefringence in Stokes space is given by

$$S_o(z) = S_o(0) \tag{18}$$

and

$$\hat{S}(z) = e^{z(\vec{\beta}x\cdot)}\cdot\vec{S}(0) = \hat{M}^{3x3}\cdot\vec{S}(0)\,. \tag{19}$$

The operator, $e^{z(\vec{\beta}x\cdot)}$, in equation (19) can be expressed in series form as

$$e^{z(\vec{\beta}x\cdot)} = \sum_n \frac{(z\beta)^n}{n!}(\vec{e}_\beta x\cdot)^n, \tag{20}$$

where $\vec{\beta}=\beta\cdot\vec{e}_\beta$.

The expansion of equation (20) results in a combination of even and odd terms which can be expressed in terms of sines and cosines. The resulting expression is

$$e^{z(\vec{\beta}x\cdot)} = \hat{M}_\beta^{3x3}(z) = \vec{e}_\beta\vec{e}_\beta + [1-\vec{e}_\beta\vec{e}_\beta]\cos(\phi) + (\vec{e}_\beta x\cdot)\sin(\phi)\,, \tag{21}$$

where $\phi = \beta z$.

The above results, equations (17) - (20), can be written in a convenient matrix form as

$$\begin{pmatrix} S_0(z) \\ S_1(z) \\ S_2(z) \\ S_3(z) \end{pmatrix} = \begin{pmatrix} 1 & 0 & 0 & 0 \\ 0 & & & \\ 0 & & \hat{M}_\beta^{3x3}(z) & \\ 0 & & & \end{pmatrix} \cdot \begin{pmatrix} S_0(0) \\ S_1(0) \\ S_2(0) \\ S_3(0) \end{pmatrix}. \qquad (22)$$

The theoretical formalism described above, which utilizes the Stokes vectors and Mueller matrices, has proven to be a powerful mathematical tool to simulate and analyze actual experimental set-ups.[9,15]

CHAPTER III

POLARIZATION, BIREFRINGENCE AND FILTER TYPES

Polarization and Birefringence

The LP_{01} mode[16] is the lowest order mode supported by a cylindrically symmetric single-mode fiber. The electric field of a single-mode optical fiber has components that are linearly polarized along the orthogonal directions as shown in figure (1). The electric fields which are associated with unperturbed and perturbed single-mode fibers were described in chapter II. For the unperturbed case, the two orthogonal modes propagate unchanged along the fiber and the SOP remains constant. On the other hand, the perturbed case, the two propagating orthogonal modes couple, which results in an evolution of the state of polarization. The evolution of the SOP continues as the light propagates along the fiber as long as the birefringence is present. After a certain length, the initial polarization state is reproduced. The length in over which this occurs is called the beat length ($L_b=2\pi/\Delta\beta$), which is inversely proportional to the birefringence. Also, the phase retardance, which is proportional to the birefringence, is given by

$$\phi(z) = \Delta\beta z. \tag{23}$$

A linearly polarized single-mode fiber with intrinsic birefringence (greater than all expected extrinsic

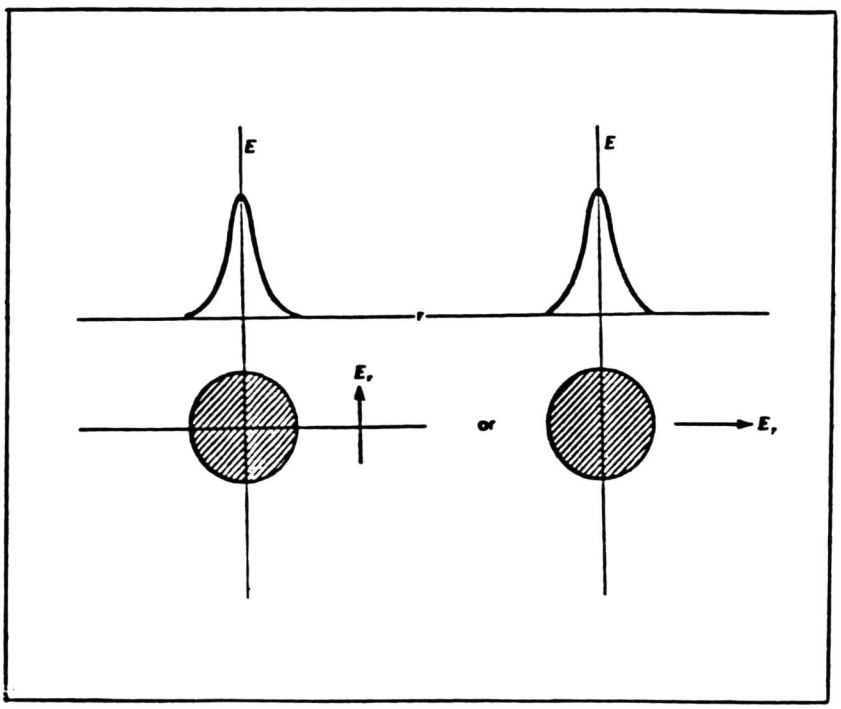

Fig. 1. Field distribution of LP_{01} mode.

birefringences) is called a polarization-maintaining fiber (PMF). There are two things that can occur when two orthogonal modes propagate along the PMF fiber. If the modes propagate on-axis, the SOP remains the same. If the modes propagate off-axis, the SOP evolves resulting in an evolution of the state of polarization as a function of the propagation length, z, and the wavelength, λ.

Circular birefringence results from external magnetic fields and twists.[8,17] The stresses created by these effects cause a coupling of the orthogonal modes, which rotates the plane of polarization of the linearly polarized light as a function of propagation length, z, and wavelength, λ. This stress-induced twist of the fiber, like those introduced during the drawing process,[18] leads to optical activity which is proportional to the twist and is expressed as

$$\Omega = g\tau, \tag{24}$$

where $g = -n_o^2 P_{44}$, $P_{44} = -.075$[19] and $n_o = 1.46$ for fused silica. Here, P_{44} is the element describing the photo-elasticity of the medium, τ is the twist-rate and n_o is the effective index of refraction for the unperturbed state.

Filter Types

One interesting application of the effects of a birefringent medium on polarized light is the birefringent filter. The Lyot and Solc filters, which are named after

their inventors,[3] are two classic birefringent filter designs.

The Lyot filter[20] is the most well-known type of birefringent filter. This filter consists of a series of linear birefringent waveplates which are sandwiched between polarizers as shown in figure (2). The lengths of the waveplates have the ratio 1:2:4:,...,:2N. Therefore, each waveplate exhibits twice the retardance of the previous one.[21] The resultant spectra of this filter is just the product of each spectra for each waveplate, as seen in figure (3). For example, in figure (3) the product of A and B results in D and the product of A, B and C results in E.

The Solc filter is another classic filter. This filter consists of a pile of linear retardation plates of birefringent material sandwiched between an input and output polarizer as shown in figure (4). Each element is oriented at a different angle depending upon the number of elements.

For the fan Solc filter, the birefringent elements are oriented in a fan-like manner and the polarizers are parallel. The angle in which the birefringent elements are oriented is given by the expression

$$\alpha = \frac{45^\circ}{N}, \tag{25}$$

where N is the number of waveplates.

For a three-stage fan filter, the elements would be oriented

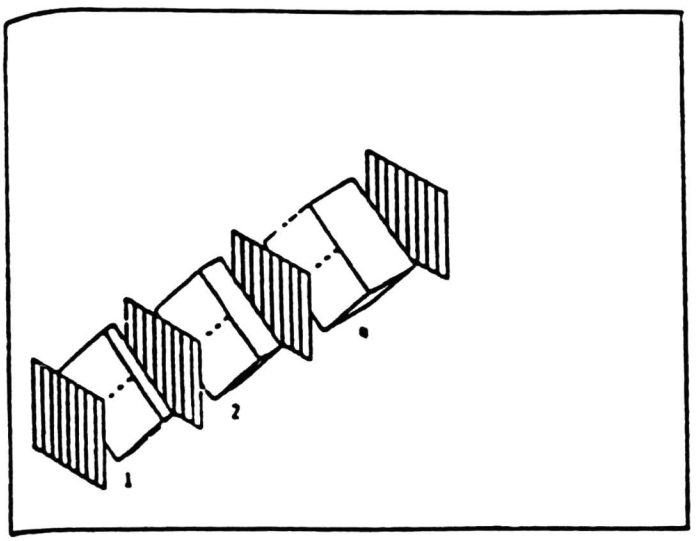

Fig. 2. 3-stage Lyot filter.

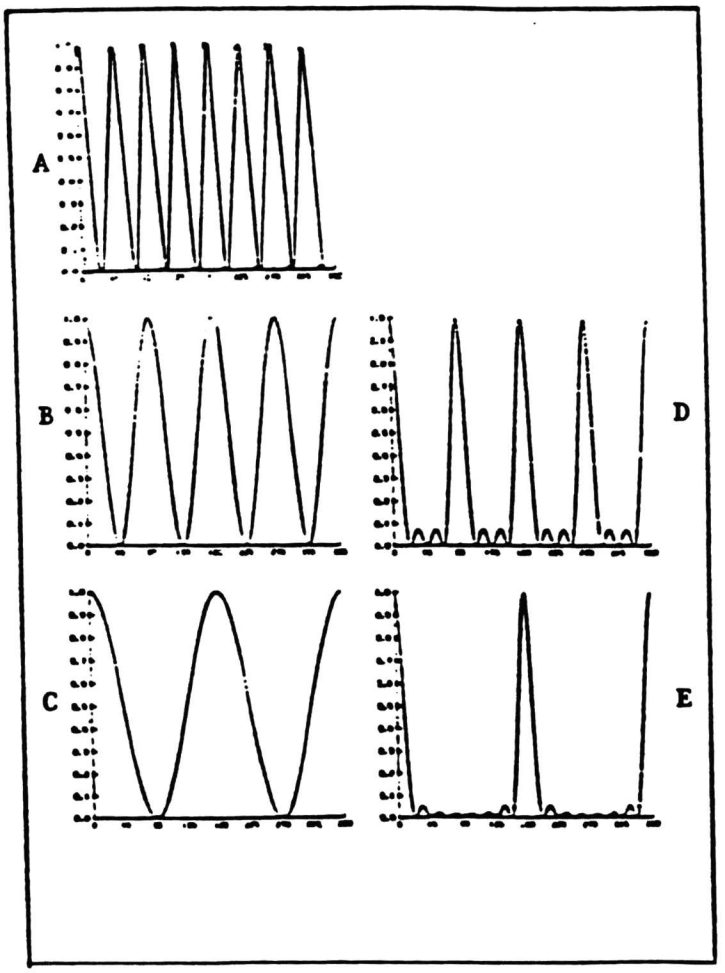

Fig. 3. Transmission versus frequency for the components of a 3-stage Lyot filter (A, B, C, D, E) through each stage.

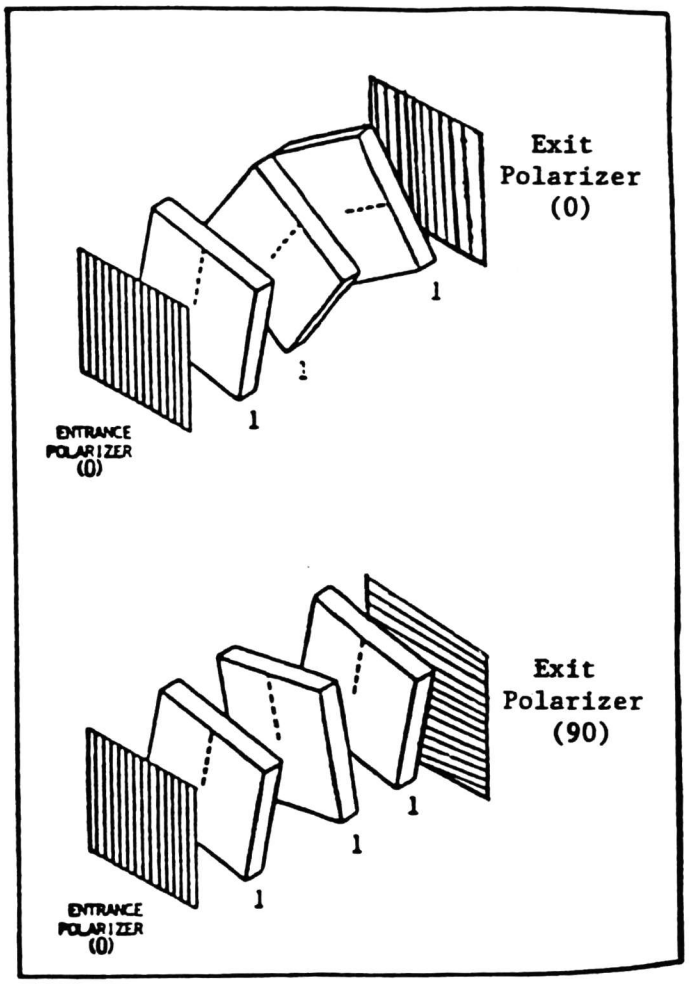

Fig. 4. Configurations of a 3-stage Solc fan and folded filter.

at angles 15°, 45° and 75°, respectively.

The folded Solc filter's birefringent elements are alternately oriented. For example, in a three-stage filter, the elements would be oriented at angles 15°, -15° and 15°. The input and output polarizers are crossed while the input polarizer is oriented at 0°. Both forms of the Solc filter worked best[3] when its elements were oriented using equation (25).

In comparing the Lyot and Solc filters, the Lyot had slightly lower sidelobes than the Solc of equal bandwidth. Therefore, Harris et al[22] developed a mathematical technique that would allow a Solc filter to duplicate the transmission profile of a similar Lyot filter. The angles for a three-stage Solc filter would be approximately 19.08°, 45° and 70.91°, respectively. So, by setting a three-stage Solc filter to the above angles, the spectra of a two-stage Lyot filter is achieved.

In fiber optic systems, the birefringent waveplates of the conventional Solc and Lyot filters are replaced by sections of fiber to perform the filtering operations.[2] Therefore, the Solc filter is more suitable for many applications because only two polarizers are required.

Tuning Techniques

Of the various tuning mechanisms discussed in chapter I, only the elasto-optical method is discussed in detail here. The Fabry-Perot method involves changing the optical path length of the light as it propagates. The quarter-wave

plates method acts as a compensator for each birefringent element of the filter by shifting the fast and slow modes out of phase by a specific amount. Also, the electro-optic method perturbs the linear birefringence and adjusts the retardance of the elements by introducing a variable electric field. In this work, we propose an the elasto-optical method utilizing twist birefringence to induce a small change in the beat length and thus tune birefringent filters.

This new elasto-optic method involves twisting each stage of the birefringent fiber filter to induce an usable phase shift. This twisting modifies the polarization state of the PMF by introducing an optical activity. While this results in an increased degradation of the side-bands of the spectra for this birefringent filter as the twist birefringence is increased, a narrow but usable tuning range can be achieved.

In comparing these tuning methods, only the elasto-optic method utilizing twist birefringence offers a simple, passive and in-line device with adjustability.

CHAPTER IV

PHYSICAL MODEL

Prototype

The model used in the search for a physical mechanism to tune an optical fiber filter using twist birefringence is shown in figure (5). Light of variable wavelength passes through an input linear polarizer, then impinges on a three-stage birefringent PMF non-dichroic fiber filter where each stage is oriented at θ_1, θ_2 and θ_3 approximately 19.08°, 45° and 70.91°, respectively. The propagating light exits through a linear polarizer that is parallel to the input polarizer and is detected by a polarization-insensitive photodetector. Utilizing the Stokes vectors and Mueller matrices, the optical components of figure (5) are multiplied (see appendix C) to give the expression

$$D = \tfrac{1}{2}\,[1 + a_3(a_2a_1 + f_2d_1 + h_2e_1) + f_3(d_2a_1 + b_2d_1 + i_2e_1) + h_3(e_2a_1 + g_2d_1 + c_2e_1)]\,, \tag{26}$$

where the matrix elements are

$$a_i = \dot{M}^i_{11} = \cos(\beta z) + (1-\cos(\beta z))\cos^2(2\theta_i)\sin^2(2\phi_i)\,,$$

$$b_i = \dot{M}^i_{22} = \cos(\beta z) + (1-\cos(\beta z))\sin^2(2\theta_i)\sin^2(2\phi_i)\,,$$

$$c_i = \dot{M}^i_{33} = \cos(\beta z) + (1-\cos(\beta z))\cos^2(2\phi_i)\,,$$

$$
\begin{aligned}
d_i &= \hat{M}^i_{21} = 1/2\ \sin(4\theta_i)\sin(2\phi_i)(1-\cos(\beta z)) \\
&\quad -\sin(\beta z)\cos(2\phi_i), \\
e_i &= \hat{M}^i_{31} = 1/2\sin(4\phi)\cos(2\theta_i)(1-\cos(\beta z)) \\
&\quad +\sin(\beta z)\sin(2\theta_i)\sin(2\phi_i), \\
f_i &= \hat{M}^i_{12} = 1/2\ \sin(2\theta_i)\sin(2\phi_i)(1-\cos(\beta z)) \\
&\quad +\sin(\beta z)\cos(2\phi_i), \\
g_i &= \hat{M}^i_{32} = 1/2\ \sin(4\phi_i)\sin(2\theta_i)(1-\cos(\beta z)) \\
&\quad -\sin(\beta z)\cos(2\theta_i)\sin(2\phi_i), \\
h_i &= \hat{M}^i_{13} = 1/2\ \sin(4\phi)\cos(2\theta_i)(1-\cos(\beta z)) \\
&\quad -\sin(\beta z)\sin(2\theta_i)\sin(2\phi_i), \\
I_i &= \hat{M}^i_{23} = 1/2\ \sin(4\phi)\sin(2\theta_i)(1-\cos(\beta z)) \\
&\quad +\sin(\beta z)\cos(2\theta_i)\sin(2\phi_i),
\end{aligned}
\tag{27}
$$

where, i = 1,.., 3. The resultant spectra of this three-stage filter is shown in figure (6). The derivation of the matrix elements is shown in appendix D. Equation (26) can be transformed into a fourier series representation utilizing a method developed by Brown et al.[23] Using this method, N stages of a Solc-like filter are multiplied and use is made of vector algebra to arrive at an expression for the fourier form of the detected power from an N stage Solc filter. The general expression can be written as

$$
D = A_0 + \sum_n A_n \cos[n(\beta z)] + \sum_n B_n \sin[n(\beta z)]. \tag{28}
$$

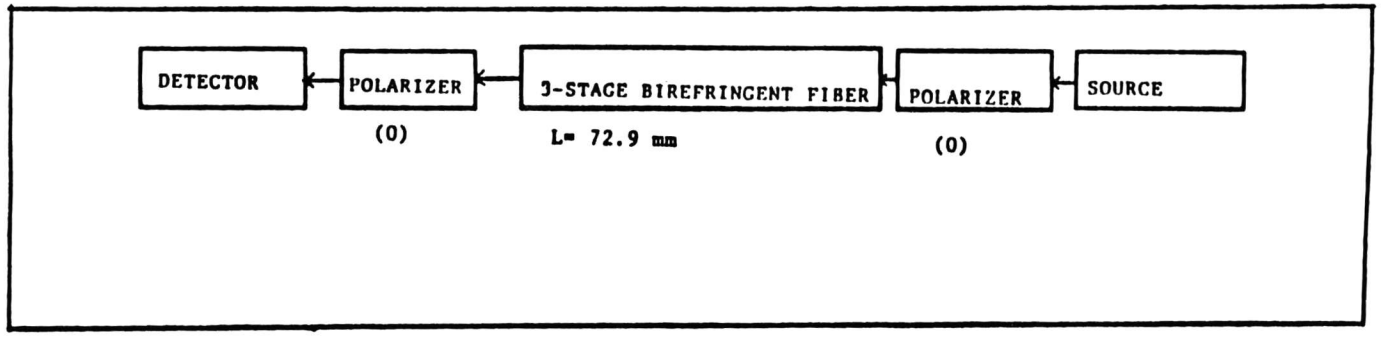

Fig. 5. Experimental set-up for 3-Stage Solc filter.

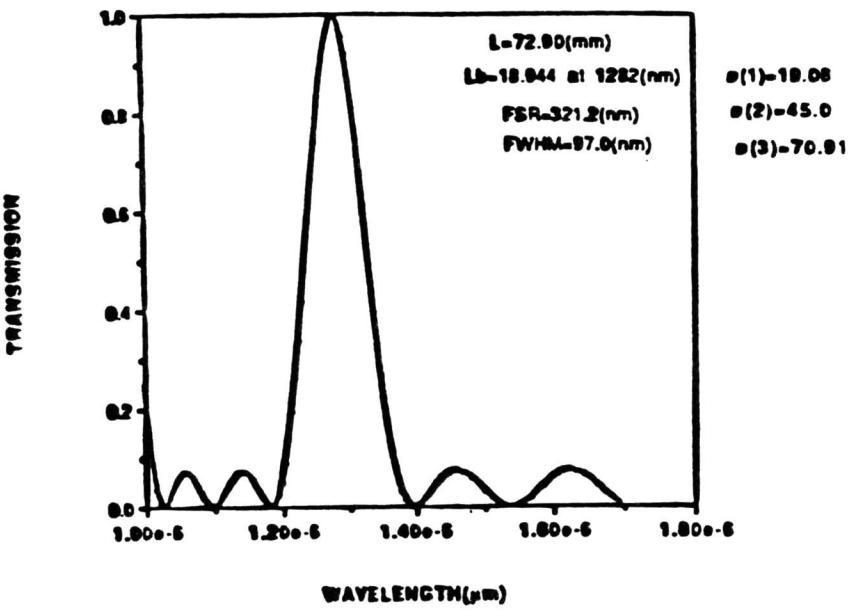

Fig. 6 Transmission versus wavelength for a 3-stage Solc filter where each stage is oriented at angles which yield a 2-stage Lyot transmission spectra.

Here, A_o is the coefficient for all terms that are independent of the retardance, A_n is the coefficient for the n^{th} cosine term and B_n is the coefficient for the n^{th} sine term. Each coefficient $\{A_o, A_n, B_n\}$ contains completed sine and cosine functions of the angles between the stages. Since the detected spectra (equation 28) is a periodic function (i.e., $D(\beta z) = D(\beta z + \phi)$), it suggests the retardance due to any tuning mechanism must be introduced to each stage. Therefore, for Solc designs, each stage of the fiber filter must be twisted or perturbed at the same rate to achieve tuning.

Analysis

When the PMF was twisted, it was found that the retardance had to be 1.75 rad or greater in order for significant tuning to be achieved. Figure (7) gives the actual spectra of this PMF filter as the twist birefringence is increased. In figure (7a), a retardance of 3.25 rad was applied to the fiber and a tuning range of 11.5 nm and a twist-rate of 7.1 rev/m was achieved. For figures (7b) and (7c), a retardance of 4.25 rad and 5.25 rad were applied to the fiber and a tuning range of 19.7 nm and 30.3 nm and a twist-rate of 9.3 rev/m and 11.5 rev/m, respectively, were achieved. A retardance of 6.25 rad was the maximum chosen for figure (7d), since the actual limitations of this fiber are unknown and a twist-rate of 13.6 rev/m seemed reasonable for a linear birefringent PMF with beat length, L_b= 18.944

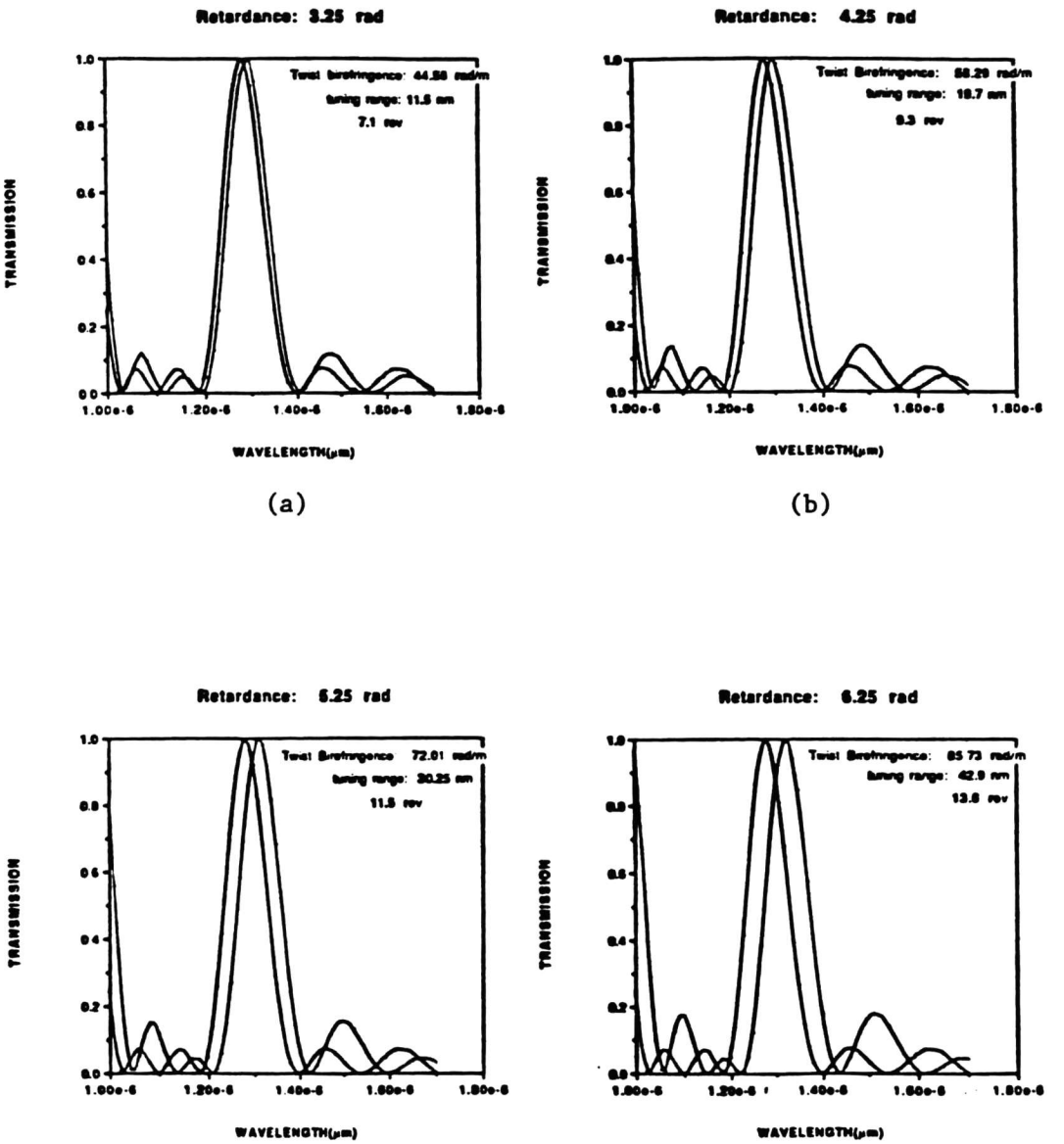

Fig. 7. Spectra of 3-Stage Solc filter as twist birefringence is increased.

mm at 1282 nm. The sidebands exhibited a maximum distortion of about 19% when a tuning range of 43 nm was achieved.

Figure (8) shows a typical set of data for tuning range versus twist birefringence. For this specific model, it was determined that when the twist birefringence was greater than 20 rad/m, the amount of twist birefringence needed to induce tuning was greatly decreased.

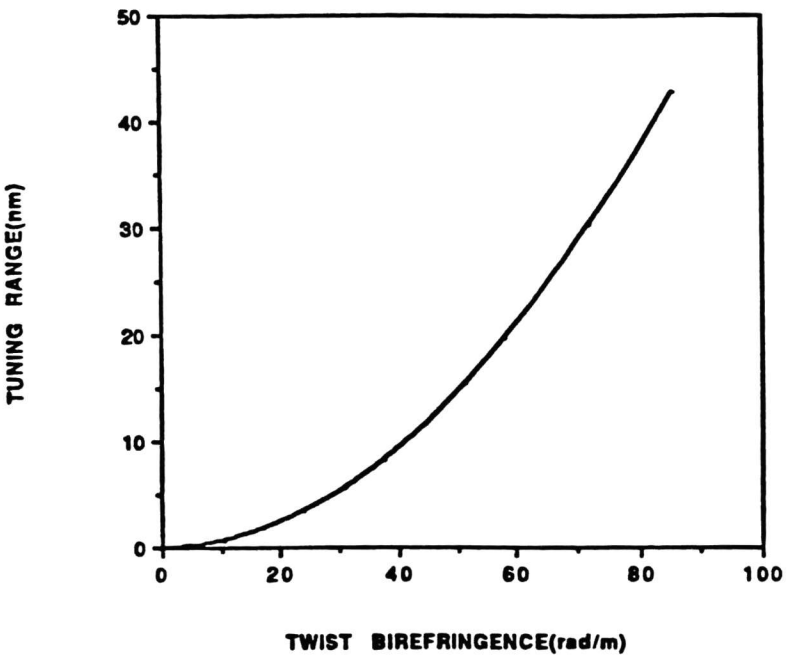

Fig. 8. Tuning range of 3-Stage Solc filter versus twist birefringence.

CHAPTER V

CONCLUSIONS AND RECOMMENDATIONS

Conclusions

In this thesis, we demonstrate using a computer simulation that twist birefringence applied to each stage tunes a spectra of an optical fiber filter over a narrow but usable range. This tuning mechanism, again, is limited by the degradation of the sidebands. Also, this tuning mechanism only allows tuning to be achieved in one direction. The maximum tuning range achieved using this mechanism was 43 nm when a twist of 13.6 rev/m was applied to the fiber filter. This particular filter could allow about fifteen channels to be tuned assuming each channel has a 2 mm width and a 2 nm separation between channel signals. The tuning limitations of this filter depend on the photo-elastic properties of the fiber and must be determined in a laboratory setting.

In comparing this tuning mechanism with the quarter-wave, electro-optic and Fabry-Perot techniques, all of the methods, except for the elasto-optic technique, needed the extensive and expensive electronics to achieve tuning. The elasto-optic method, however, requires only the manual twisting of each stage of the filter to achieve tuning.

Recommendations

I highly recommend this tunable filter design for fabrication be a future thesis topic. Once it is

fabricated, the detailed characterization of the tunability could be done and compared with the simulations developed here.

APPENDIX A: Z-ordered exponential operator.[11]

Consider

$$\hat{M} = \underset{\leftarrow}{Z} \exp\left[\int_{z_0}^{z} \hat{m}(z')dz'\right], \tag{A1}$$

where the $\underset{\leftarrow}{Z}$ signifies z ordering such that all greater distances are ordered to the left. That is,

$$\underset{\leftarrow}{Z} \exp\left[\int_{z_0}^{z} \hat{m}(z')dz'\right] = \hat{1} + \sum_{n} \int_{z_0}^{z} dz_1 \int_{z_0}^{z} dz_2 \cdots \int_{z_0}^{z_{n-1}} dz_n \left[(\hat{m}(z_1)\hat{m}(z_2)\cdots\hat{m}(z_n)\right]. \tag{A2}$$

This operation properly accounts for the possible non-communitivity of the operators at different distances along z.

APPENDIX B. Pauli Spin Matrices

$$\hat{\sigma}_0 = \begin{pmatrix} 1 & 0 \\ 0 & 1 \end{pmatrix} \tag{B1}$$

$$\hat{\sigma}_1 = \begin{pmatrix} 0 & 1 \\ 1 & 0 \end{pmatrix} \tag{B2}$$

$$\hat{\sigma}_2 = \begin{pmatrix} 1 & 0 \\ 0 & -1 \end{pmatrix} \tag{B3}$$

$$\hat{\sigma}_3 = \begin{pmatrix} 0 & -i \\ +i & 0 \end{pmatrix} \tag{B4}$$

APPENDIX C. Matrices for Optical Components.

$$P_{input} = P_{output} = \begin{pmatrix} 1 & 1 & 0 & 0 \\ 1 & 1 & 0 & 0 \\ 0 & 0 & 0 & 0 \\ 0 & 0 & 0 & 0 \end{pmatrix} \tag{C1}$$

$$Source = \begin{pmatrix} 1 \\ 1 \\ 0 \\ 0 \end{pmatrix} \tag{C2}$$

$$Detector = \overbrace{1 \quad 0 \quad 0 \quad 0} \tag{C3}$$

$$3\text{-}Stage\ Fiber = \begin{pmatrix} 1 & 0 & 0 & 0 \\ 0 & A_i & F_i & H_i \\ 0 & D_i & B_i & I_i \\ 0 & E_i & G_i & C_i \end{pmatrix} \quad (i = 1,2,3) \tag{C4}$$

For figure (5), the optical components would be positioned as:

$$D = \begin{pmatrix} 1 \\ 0 \\ 0 \\ 0 \end{pmatrix} \cdot \begin{pmatrix} 1 & 1 & 0 & 0 \\ 1 & 1 & 0 & 0 \\ 0 & 0 & 0 & 0 \\ 0 & 0 & 0 & 0 \end{pmatrix} \cdot \begin{pmatrix} 1 & 0 & 0 & 0 \\ 0 & a_3 & f_3 & h_3 \\ 0 & d_3 & b_3 & i_3 \\ 0 & e_3 & g_3 & c_3 \end{pmatrix} \cdot \begin{pmatrix} 1 & 0 & 0 & 0 \\ 0 & a_2 & f_2 & h_2 \\ 0 & d_2 & b_2 & i_2 \\ 0 & e_2 & g_2 & c_2 \end{pmatrix} \cdot \begin{pmatrix} 1 & 0 & 0 & 0 \\ 0 & a_1 & f_1 & h_1 \\ 0 & d_1 & b_1 & i_1 \\ 0 & e_1 & g_1 & c_1 \end{pmatrix} \cdot \begin{pmatrix} 1 & 1 & 0 & 0 \\ 1 & 1 & 0 & 0 \\ 0 & 0 & 0 & 0 \\ 0 & 0 & 0 & 0 \end{pmatrix} \cdot \begin{pmatrix} 1 \\ 1 \\ 0 \\ 0 \end{pmatrix} \tag{C5}$$

which after some algebra, becomes equation (26).

APPENDIX D: Derivation of Matrix Elements.

Given the equation

$$\hat{M}_G^{3x3} = \cos(\beta z) + (1-\cos(\beta z))\,\vec{e}_\beta \vec{e}_\beta + (\hat{e}_\beta x \cdot)\sin(\beta z), \qquad (D1)$$

the matrix elements of a 3-dimensional system in Stokes space can be derived. First, let

$$\vec{e}_\beta = \sum_l \alpha_l \vec{e}_l = \left(\frac{\vec{\beta}}{\beta}\right) = \left(\frac{\beta_1}{\beta}\right)\vec{e}_1 + \left(\frac{\beta_2}{\beta}\right)\vec{e}_2 + \left(\frac{\beta_3}{\beta}\right)\vec{e}_3 \qquad (D2)$$

where $\alpha_l = (\beta_l/\beta)$, $\beta = (\beta_1^2 + \beta_3^2)^{1/2}$, $\vec{e}_\beta = \cos(2\theta)\sin(2\phi)\vec{e}_1 + \sin(2\theta)\sin(2\phi)\vec{e}_2 + \cos(2\phi)\vec{e}_3$ and $\phi = \frac{1}{2}\cos^{-1}(\beta_3/\beta)$. Then, let $\vec{e}_\beta$ operate on eq. (D1) which becomes

$$\hat{M}_{ii}^{3x3} = \cos(\beta z) + (1-\cos(\beta z))\,\alpha_j^2; \text{ for } i=j \qquad (D3)$$

and

$$\hat{M}_{ij}^{3x3} = (1-\cos(\beta z))\,\alpha_i\,\alpha_j + \sin(\beta z)\sum_l \alpha_l \epsilon_{ljl}; \text{ for } i \neq j. \qquad (D4)$$

REFERENCES

1. A. M. Title and S. A. Schoolman, SPIE Polarized Light, 88, pp. 23-25 (1976).

2. A. M. Title and N. J. Rosenberg, Optical Engineering 20, pp. 815-823 (1981).

3. J. Evans, Opt. Soc. Am., 48, No. 3, 142 (1958).

4. R.C. Jones, J. Opt. Soc. Am., 31, pp. 488-500 (1941).

5. C. S. Brown, To be published.

6. D. Marcuse, Theory of Dielectric Optical Waveguides (Academy Press; New York; 1974).

7. C. S. Brown and A. Teate, To be published.

8. Simon and Ulrich, Appl. Opt., 18, pp. 2241-2251 (1979).

9. C. S. Brown, SPIE Polarization Considerations for Optical Systems II, 1166, 155 (1989).

10. M. Born and E. Wolf, Principles of Optics (Pergamon Press; New York; 1975); Chapter 10.

11. R. F. Fox, Physics Reports, 48, No. 3, 238 (1978).

12. R. M. Azzam, J. Opt. Soc. Am., 68, No. 12, pp. 1756-1776 (1978).

13. S. R. Mallinson, Appl. Opt., 26, No. 3, 431 (1987).

14. R. Gilmore, Lie Groups, Lie Algebras and Some of Their Applications, (John Wiley & Sons; New York; 1974); Chapter 3.

15. M. Shute and C. Brown, J. Light. Tech., 7, No. 12, 2013 (1989).

16. S. Rashleigh, J. Light. Tech., 2, pp. 313-317 (1983).

17. H. Papp and H. Harms, Appl. Opt., 14, 2406 (1975).

18. F. M. Sears, J. Light. Tech., 8, No. 5, 686 (1990).

19. D. Gray, American Institute of Physics Handbook, (McGraw Hill; New York; 1976); pp. 6-236.

20. J. W. Evans, J. Opt. Soc. Am., 39, No. 3, 229 (1949).

21. M. Johnson, Opt. Soc. Am., 5, 142 (1980).

22. S. Harris, E. Ammann and I. Chang, J. Opt. Soc. Am., 54, 1267 (1964).

23. C.S. Brown, J.F. Kuhl, and M.A. El, Proceedings of SPIE, 988, 276 (1988).

ABSTRACT

PHYSICS

Myers, Terry W. B.S. Southern University, 1988

TUNING WAVELENGTH SELECTIVE BIREFRINGENT OPTICAL FIBER FILTERS USING TWIST BIREFRINGENCE

Advisor: Dr. Charles S. Brown

Thesis dated May, 1991

A novel physical tuning mechanism for optical fiber filters is proposed and studied. To explore tuning mechanisms, a theoretical model of a Solc birefringent fiber filter is described. The coherency equation of motion for a birefringent filter is solved by transforming to the Stokes-Mueller matrix equation via the measurable Stokes parameters. The Mueller matrix is then expanded in a Taylor series using the generators of the Lorentz transformations. The Stokes vectors and Mueller matrices provide a theoretical formalism which is used to simulate an experimental set-up and to describe the transmission of light through a birefringent fiber filter system. Hence, the theoretical expression for the transmission spectra incident on a detector is derived. This expression is then transformed to the more convenient fourier series form. This form is used to determine the particular type of perturbation necessary to tune a filter. Specifically, a tuning mechanism utilizing twist birefringence is proposed

and analyzed. Moreover, we show using theoretical and computer simulation studies that twist birefringence tunes a filter spectra over a narrow but usable range, provided each stage in the filter is twisted at the same rate. For example, a twist birefringence of 85.7 rad/m generated a 42.8 nm tuning range on the filter spectra of a three-stage Solc-type fiber filter when each optical fiber stage is linearly birefringent with a beat length of 18.94 mm at 1282 nm.

ABSTRACT

PHYSICS

Myers, Terry W. B.S. Southern University, 1988

TUNING WAVELENGTH SELECTIVE BIREFRINGENT OPTICAL FIBER FILTERS USING TWIST BIREFRINGENCE

Advisor: Dr. Charles S. Brown

Thesis dated May, 1991

A novel physical tuning mechanism for optical fiber filters is proposed and studied. To explore tuning mechanisms, a theoretical model of a Solc birefringent fiber filter is described. The coherency equation of motion for a birefringent filter is solved by transforming to the Stokes-Mueller matrix equation via the measurable Stokes parameters. The Mueller matrix is then expanded in a Taylor series using the generators of the Lorentz transformations. The Stokes vectors and Mueller matrices provide a theoretical formalism which is used to simulate an experimental set-up and to describe the transmission of light through a birefringent fiber filter system. Hence, the theoretical expression for the transmission spectra incident on a detector is derived. This expression is then transformed to the more convenient fourier series form. This form is used to determine the particular type of perturbation necessary to tune a filter. Specifically, a tuning mechanism utilizing twist birefringence is proposed

and analyzed. Moreover, we show using theoretical and computer simulation studies that twist birefringence tunes a filter spectra over a narrow but usable range, provided each stage in the filter is twisted at the same rate. For example, a twist birefringence of 85.7 rad/m generated a 42.8 nm tuning range on the filter spectra of a three-stage Solc-type fiber filter when each optical fiber stage is linearly birefringent with a beat length of 18.94 mm at 1282 nm.

58-2
T-688